

Size Reduction of a DC Link Choke Using Saturation Gap and Biasing with Permanent Magnets

Aguilar, Andres Revilla; Munk-Nielsen, Stig; Zuccherato, Marco; Thougard, Hans-Jørgen

Published in:

PCIM Europe 2014. International Exhibition and Conference for Power Electronics, Intelligent Motion, Renewable Energy and Energy Management Nuremberg, 20 – 22 May 2014, Proceedings

Publication date:
2014

Document Version
Early version, also known as pre-print

[Link to publication from Aalborg University](#)

Citation for published version (APA):

Aguilar, A. R., Munk-Nielsen, S., Zuccherato, M., & Thougard, H.-J. (2014). Size Reduction of a DC Link Choke Using Saturation Gap and Biasing with Permanent Magnets. In PCIM Europe 2014. International Exhibition and Conference for Power Electronics, Intelligent Motion, Renewable Energy and Energy Management Nuremberg, 20 – 22 May 2014, Proceedings (pp. 1667-1674). VDE Verlag GMBH.

General rights

Copyright and moral rights for the publications made accessible in the public portal are retained by the authors and/or other copyright owners and it is a condition of accessing publications that users recognise and abide by the legal requirements associated with these rights.

- Users may download and print one copy of any publication from the public portal for the purpose of private study or research.
- You may not further distribute the material or use it for any profit-making activity or commercial gain
- You may freely distribute the URL identifying the publication in the public portal -

Take down policy

If you believe that this document breaches copyright please contact us at vbn@aub.aau.dk providing details, and we will remove access to the work immediately and investigate your claim.

Size Reduction of a DC link Choke Using Saturation-gap and Biasing with Permanent Magnets

Andrés, Revilla Aguilar, Aalborg University, Denmark, are@et.aau.dk

Stig, Munk-Nielsen, Aalborg University, Denmark, smn@et.aau.dk

Marco, Zuccherato, Danfoss Power Electronics, Denmark, Marco.Zuccherato@danfoss.com

Hans-Jørgen, Thougard, Sintex, Denmark, hjt-sintex@grundfos.com

Abstract

This document describes the design procedure of permanent magnet biased DC inductors using the *Saturation-gap* technique [1]. This biasing configuration can provide a 50% reduction in either the core volume or the number of turns, while meeting its current and inductance requirements. A design example on a 20A 1mH iron laminations DC choke is presented. MEC simulations and empirical measurements on a physical unit were performed. Experimental results show a 50% reduction of the core volume is achieved. The total volume reduction of the inductor is 37%.

1. Introduction

The use of permanent magnets for introducing bias magnetization in DC inductors is a known technique for extending the saturation current limit and accordingly reducing the required inductor's size. The first designs of hybrid inductors presented the magnet inserted in the air-gap [2][3]. This configuration can introduce a certain amount of bias flux; on the other hand the magnet size is limited by the air-gap size, presenting limitations on the inductor design. More recent designs uses nonstandard core shapes with magnets in the vicinity of the air-gaps [4][5]. These configurations can achieve a higher level of bias flux; on the other hand the requirement of specially design core shapes may be an important disadvantage.

The saturation-gap [1] configuration can be implemented with standard non-gaped UI iron laminations and can achieve 100% bias flux. Fig.1. shows the basic core and magnets arrangement of the saturation-gap configuration. The red vectors represents the flux from the coil, green vectors represents flux from the magnets. The function of the permanent magnets in this configuration is a twofold: to produce saturation in a localized segment of the core which will behave as a variable virtual air gap and to create a biasing flux in the rest of the core.

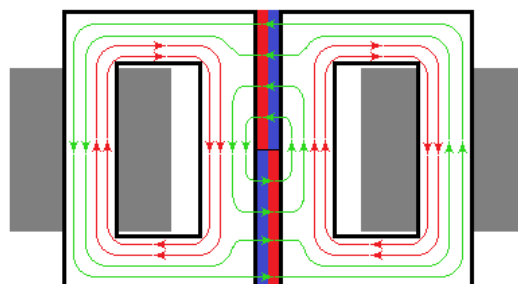


Fig. 1. . Saturation-gap biasing configuration. Red vectors represent flux produced by the coils. Green vectors represent flux produced by the magnets. Vectors in opposite direction represents biasing. Vectors in the same direction represents saturation-gap.

The following section II will present an inductor design strategy based on the saturation-gap configuration. A design example of 50% core reduction on a standard choke will also be presented.

Section III will present Magnetic Equivalent Circuit (MEC) simulation of the proposed solution. Section IV will present the experimental analysis measured on the physically build hybrid and the standard chokes. Finally section V will present the conclusions and further work.

2. Design Strategy

Any given standard EI (or EE) inductor design can be improved by using two UI (or UU) cores in saturation-gap configuration. This section describes the generic procedure for reducing the size and/or the copper losses of a given DC inductor, using the saturation-gap biasing configuration. A specific design example targeting 50% core size reduction of an EI66 1mH 20A DC link choke is also presented.

2.1. Introduction to Saturation-gap Inductor Design

The basic formula used for inductor size calculations is:

$$L I = N B_{sat} A_c$$

Where L is inductance, I is the current, N is the number of turns, A_c is the area cross section of the core and B_{sat} is the saturation flux density of the material. In the following, when no additional sub-indexes are attached to these variables, they will refer to the standardised EI core parameters. When referring to the variables of either the hybrid inductor or the individual UI cores, the $_h$ and $_{UI}$ sub-indexes will be used.

In the left hand of the equation we have the variables, directly related to the target inductor specifications. In the right hand of the equation we have the parameters related to the choke geometry and material characteristics. The product of these parameters will represent a constant. This design constant will define the maximum LI product achievable of each inductor design. The specific nominal inductance L_N is adjusted by the length and shape of the air-gap. The blue line in Fig. 2. represents the LI product region of a generic unity value design constant. Constant length air-gaps produce constant L_N as a function of current until crossing the LI product region. At this point it is defined the saturation current I_{Sat} of the inductor. The use of stepped or non-constant length air-gaps will produce nonlinear inductance profiles. This can maximize the working region of an inductor within a given LI design constant.

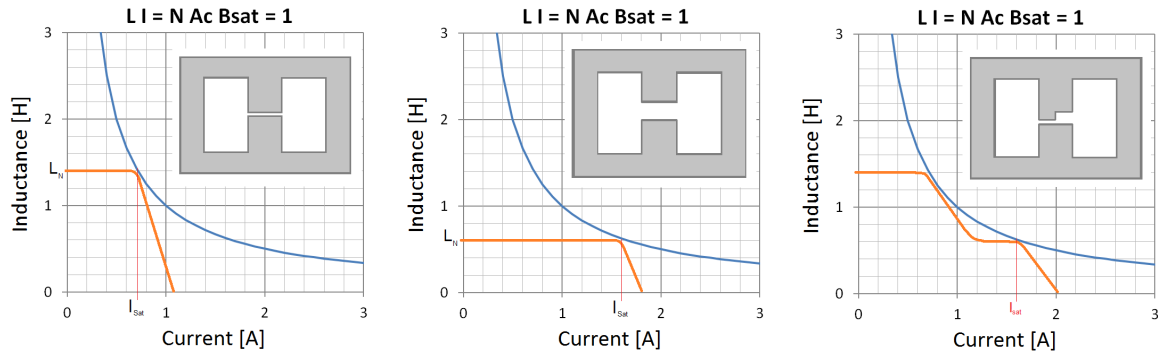


Fig. 2. . Inductor's working range as a function of gap dimensions. Blue curve is a unity LI product region. Orange curve represents the inductance versus current profile for each air-gap. Left: Short air-gap; Middle: Long air-gap; Right: Nonlinear gap.

The saturation-gap configuration, presented in Fig. 1, does not use physical air-gaps. The equivalent reluctance of an air-gap is induced in a segment of each core, by means of partial saturation. The length and shape of the induced equivalent air-gap is a complex function involving: the core saturation profile; the instantaneous flux levels produced by coils and magnets; and the magnets and cores relative geometry.

Permanent magnets behaviour can be simulated as a constant mmf source with a series internal reluctance. The instantaneous flux produced by the magnet is inversely proportional to the reluctance

of its magnetic path. The minimum and maximum flux levels produced by a magnet are defined by its length M_L and area cross-section A_{cM} respectively [6]. The flux level produced by the permanent magnets in the present configuration, is continuously adapting to the variations induced by the coil's flux, maintaining a Quasi-Saturated Equilibrium (QSE) in the saturation-gap region.

For the biasing of laminated iron cores a high flux density permanent magnet material needs to be used. The chosen material is Neodymium Iron Boron, NdFeB with $B_r = 1.2 \text{ T}$. As a rough approximation we can suppose the maximum flux density B_r of the NdFeB magnets, to be equivalent to the saturation level of the laminated iron. In order to fully bias the inductor and to bring the saturation-gap region to an almost-saturated state, the permanent magnet needs to provide enough flux for the two flux paths (the saturation-gap path and the biasing path). Accordingly, the area cross-section of the magnets A_{cM} , needs to be at least two times the area cross-section of the core A_c .

$$A_{cM} / A_c > 2$$

The A_{cM} / A_c ratio of standard UI laminations is equal to 2.5. By using UU laminations the ratio can be increased up to 4. Since the hybrid inductor is composed of two UI cores connected in series, the inductance requirement for each UI core is half of the standard inductor. That provides an extra reduction factor of 2 in the design of the UI cores. Both UI cores will contribute equally to the total volume of the inductor. Accordingly this extra reduction factor is applied to the required A_{cUI} in order to maintain the volume proportion of the total hybrid core.

$$A_{cUI} = A_{ch} / 2$$

By reducing A_{cUI} , the required winding turn length is also reduced. If the applied reduction factor is performed with equal rectangular proportion R_{Ac} , the wire length is been reduced by the same proportion. The perfect square proportion ($R_{Ac}=1$) will provide the shortest wire length. Assuming full bias is achieved, we can extend the max flux density of the hybrid inductor to double the B_{sat} value of the material. Accordingly, we have the possibility of reducing N_h or A_{ch} by a factor of 2, while meeting the same current and inductance requirements.

$$L I = L_h I_h = N_h A_{ch} 2B_{sat}$$

$$N_h A_{ch} = N A_c / 2$$

The focus of the specific design strategy should be used in order to decide the distribution of the reduction factor. Applications using a high DC current could benefit from a reduction in copper resistance and increase the efficiency. On the other hand, many designs require smaller and lighter cores.

Using the entire reduction factor for the area cross-section A_c will allow for the use of the smallest core and decrease the component weight. On the other hand, the required window area, W_a will remain the same. In this situation is possible to use the equivalent W_a size of UI laminations ($2 \times \text{UI} = \text{EI}$), and reduce the laminations stack length, L_{stack} by half. This procedure is illustrated in Fig. 3. Another possible procedure could be to replace one bigger EI core with two smaller UU cores.

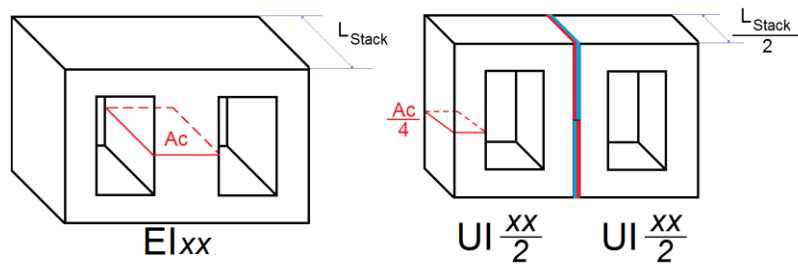


Fig. 3. Half core volume reduction strategy with saturation-gap hybrid configuration.

Using the entire reduction factor for the number of turns N will decrease the wire resistance and the required window area by a factor of two, allowing for core size reduction or bigger wire cross-section for additional reduction of copper resistance. Since the required window area becomes smaller while the area cross-section A_c must remain the same, this strategy can be used to replace one bigger EE core with two smaller UI cores.

A compromised distribution of the reduction factor, between A_c and N , is also possible and needed to a certain extent, in order to accommodate to the finite possible standardised lamination sizes.

2.2. Practical Design Example with Saturation-gap

The target inductor rating parameters of our standard choke are: $I=20A$, $L=1mH$, $I_{stack} = 34mm$, accordingly the area cross-section is: $A_c = 34 \times 22 = 748 \text{ mm}^2$. The number of turns is $N = 36$. The wire diameter is $\phi = 2.24 \text{ mm}$. Gap length $l_{gap} = 1.2 \text{ mm}$. The area used by the coil is $C_{wa} = 140 \text{ mm}^2$ and the total window area $W_a = 363 \text{ mm}^2$. The packing factor in the window area is $k = 0.4$.

Since the present design strategy is focused on core size reduction, it is desired to use the entire reduction factor for the cross-sectional area of the UI cores. The following formulas describe the design requirements for each UI core:

$$N_{UI} = N$$

$$A_{cUI} = A_c / 4$$

Since the required number of turns, and accordingly the window area did not change, it is recommendable choosing the UI core equivalent of half the target standard EI core ($2 \times \text{UI33} = \text{EI66}$). By using a stack length, I_{stack} equal to half of that in the standard, we achieve the required $\frac{1}{4}$ reduction of A_{cUI} , while keeping the same R_{Ac} and accordingly the total wire length. This design will present 50% core volume while keeping equal wire length and resistance. Unfortunately, UI33 laminations are not a standardized size. The closer standard UI core size found is UI30. The W_a of UI30 is slightly smaller than the standard EI66 and the same coil could fit by a small increase in the packing factor. In order to achieve the required A_{cUI} with UI30 laminations the minimum required stack thickness is calculated.

Accordingly to the previous calculation, the final UI cores specifications are: $N_{UI} = 36 \text{ turns}$; $\phi = 2.24 \text{ mm}$; $I_{stackUI} = 20mm$. The magnet specifications: $M_L = 3mm$; $A_{cM} = 20 \times 25mm$ covering all the area between UI cores. The total volume of the hybrid core (including the two UI cores) has decreased 50%. The achieved rectangular proportion of the windings is higher than desired, $R_{AcUI} = 2$, and a small increase in wire resistance is expected. By comparing the A_c perimeter length of the standard and the hybrid designs, the expected increase in wire resistance is approximately 18%.

3. Simulation Analysis

In order to verify the proposed design and to further investigate the behavior of the saturation-gap configuration a Magnetic Equivalent Circuit (MEC) model of both inductors was created using LTspice. Fig. 4. shows the MEC models of both the hybrid and the standard inductors. Each core is divided into segments. The UI segments connected to the magnets are subdivided in 9 segments in series, in order to provide a higher resolution in the saturation-gap area. The magnets are modeled as an F_{mag} (voltage) source with series reluctance R_{mag} . A parallel reluctance R_{frg} is inserted to account for fringing flux [4]. The total surface of each magnet, M_a is simulated with four smaller magnets with $\frac{1}{4}$ of

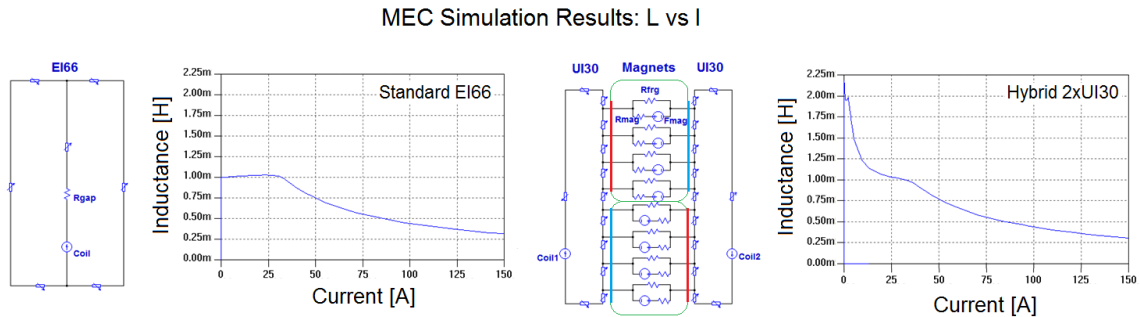


Fig. 4. Magnetic Equivalent Circuit (MEC) models and simulation results. Inductance versus current.

the original M_a , in order to match the present segment resolution. The reluctance of each core segment is simulated by a non-linear resistor. The values of these non-linear resistor's are introduced as V vs I look-up tables. The actual values were calculated using the segment dimensions and the B vs H curve found on the core specifications. Each coil is represented as a magnetic flux (current) source which is related to the electrical winding of the models as in [8]. The values of the different MEC elements were calculated using the design's geometrical specifications presented in section II, and applying the common simulation formulas as in [1][8].

The models were tested using a 20V DC pulse stimulus of 3 ms duration. The produced current and voltage waveforms were computed and the inductance value as a function of the current was calculated. The obtained results from the hybrid and standard inductors are shown next to their respective models in Fig. 4.

MEC Simulation: Voltage Pulse Test

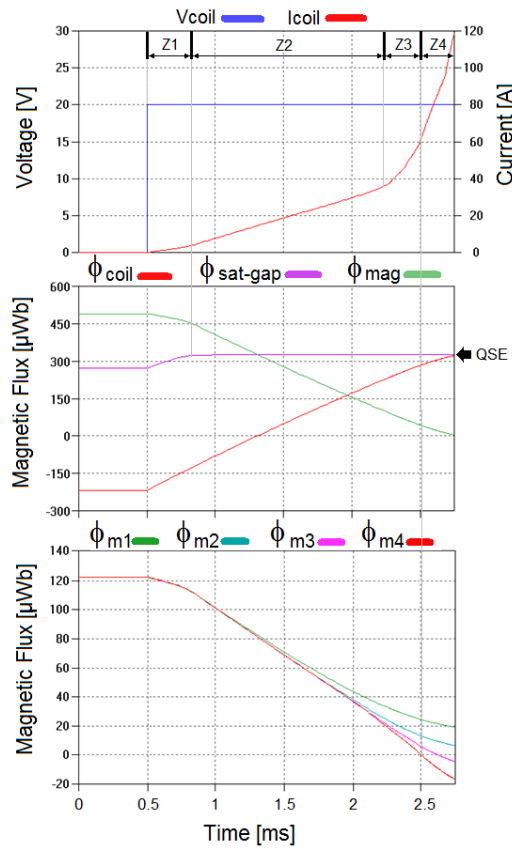


Fig. 5. MEC simulation: Voltage pulse test instantaneous signals. Top: Current and voltage at electric terminals; Middle: Magnetic flux present at coil segment (red), saturation-gap segment (purple) and at the total magnet area (green); Bottom: Magnetic flux present at each magnet segment (ϕ_{m1} is the magnet segment closest to center).

The standard choke model presents a characteristic inductance profile, having a nominal inductance, $L_n = 1$ mH. The saturation knee point appears at $I_{sat} = 30$ A, approximately. The hybrid choke model presents a nonlinear inductance profile. The saturation point and the inductance value above 20A, is perfectly matching the standard choke profile. The inductance at zero current is two times the nominal value and decreases exponentially until reaching $L_n = 1$ mH at 20A. This nonlinear inductor behavior is due to the variations of the equivalent virtual air-gap produced in the saturation-gap region.

In order to further investigate the behavior of the saturation-gap and to identify the possible tuning mechanisms, the different flux signals in the model were analyzed. Fig. 5. shows the voltage pulse stimulus and the obtained current ramp at the electrical terminals of the hybrid model. Additionally, the

instantaneous flux, ϕ [Wb] at the key points of the MEC are presented. At the top plot of Fig. 5. different current behavior zones (Z1 to Z4) are identified and delimited along the voltage pulse duration. The different zones are representative of different flux behavior within the saturation-gap and they are delimited by different current threshold values:

- **Z1. Nonlinear inductor behavior:** The flux level, present at the saturation-gap, at 0A current, has not reached the Quasi-Saturated Equilibrium (QSE) point. The initial equivalent air-gap is very short and exponentially increases as the flux from the coil is adding to the saturation-gap flux level. Accordingly, an exponential decrease in inductance is achieved.
- **Z2. Linear inductor behaviour:** The flux level, present at the saturation-gap has reached the QSE point. A linear increase of the coil's flux is equilibrated by a linear decrease of the magnet's flux, maintaining the QSE point at the saturation-gap center. The starting current threshold of this zone is controllable by the amount of magnet's flux. A bigger magnet could introduce the necessary flux to reach the QSE from the 0A current point.
- **Z3. Core saturation:** The saturation current, I_{sat} delimits the onset of this zone. The saturation-gap flux is constant at QSE and the behavior of the coil and magnet fluxes is identical as in Z2. On the other hand, the core material has reached saturation and the inductance value decreases rapidly.
- **Z4. Demagnetization threshold:** The flux produced by the magnet segment closer to the edge (ϕ_{m4}) has reached zero value. No flux is produced by this section of the magnet. As current increases, flux from the coil crosses through the magnet ending up in demagnetization effects.

The desired working point in most applications would be Z2. Nonlinear behavior zones like Z1 are in principle not desired. On the other hand, several applications using standard nonlinear-gap inductors could benefit from this configuration. The *Core saturation* threshold of the present model appears at 30 A. The *Demagnetization threshold* is not observed until reaching 60 A current. Accordingly, the magnets will not suffer demagnetization in the working current range of the hybrid inductor (Z1 to Z2).

4. Experimental Analysis

The standard and the hybrid design, presented in the previous sections, were physically implemented and compared using two different experimental tests. The first test consisted in generic inductor characterization measurements, using a Wayne Kerr magnetics analyzer. In the second test, the units were analyzed at higher power using a Spitzenberger Grid Simulator. The units were driven at nominal AC and DC Bias level, simulating the working conditions of DC link in a frequency converter.

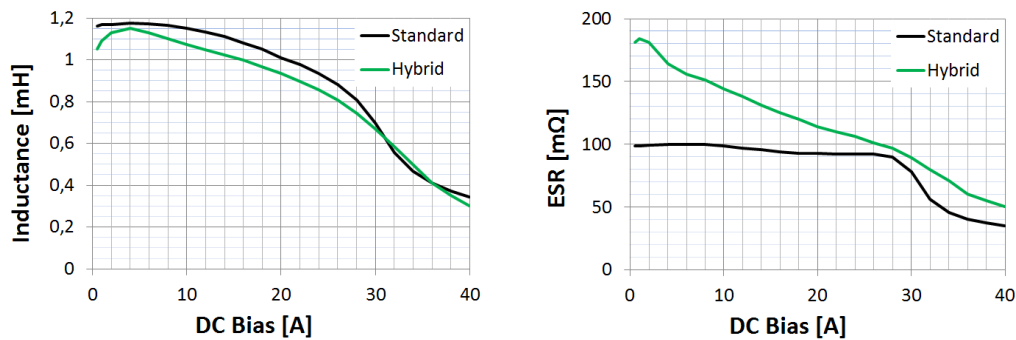


Fig. 6. Inductance versus DC bias current (top) and Equivalent Series Resistance (ESR) versus DC bias current (bottom). Measured with WK3260B magnetic analyser and WK3265B bias units. Stimulus: 1Vrms AC 300Hz.

4.1. Inductor Characterization Measurements

A Wayne Kerr 3260B Magnetics Analyser with two WK3265B bias units was used to characterise the two inductor designs. The analyser uses a low power AC voltage stimulus for measurement calculations. The two WK3265B bias units can provide adjustable DC bias current levels up to 50 A.

The inductance and the ESR (*Equivalent Series Resistance*) as a function of the DC bias current were measured for both inductors. Fig. 6. shows the obtained measurement results.

The Inductance versus DC Current Bias graph shows the comparison between the inductance value of the standard and hybrid solutions as a function of the applied DC current. The standard choke exhibits the typical inductance vs current profile of a gapped laminated steel inductor. The inductance value is maximal at the lower bias current and slowly decreases along the working current range of the inductor. At current levels higher than 28A, the inductance value is rapidly decreasing due to saturation of the core material. The hybrid choke replicates quite well the standard choke behaviour over all the DC current bias range, but shows a slightly lower inductance value for almost all the working points. It is also noticeable how the inductance value of the hybrid choke is initially increasing in the lower bias current range, reaching its maximum value at 4 A. This is contrary to the expectations of the MEC analysis. This effect is an indication of the permanent magnet biasing flux is reaching the negative saturation level of the core (Z0).

The ESR versus DC Current Bias graph shows the comparison between the ESR value of the standard and hybrid solutions as a function of the applied DC current. The measured ESR value of the choke under test represents the total power losses in the component, seen as the sum of copper losses and core losses. The measured DC winding resistance of the standard and hybrid chokes are 27 mΩ and 35 mΩ respectively. The higher copper resistance of the hybrid inductor is expected according to the design calculations provided in section II. The standard choke exhibits a flat ESR curve up to 28 A DC bias current. This is the working region of the core and losses are almost constant. At 28 A DC bias current, the laminated core material starts saturating and gradually reduces the contribution of the core losses in the choke, leading to decreasing values of the measured ESR. The hybrid choke presents an unexpected loss profile. The ESR value is maximal at low DC current levels, and decreases constantly as the DC current increases. At the nominal DC current level (20 A) the ESR value of the hybrid inductor is 20% higher than that of the standard choke and at the saturation point (28 A) the ESR value is only a 10% higher.

4.2. Nominal Power AC +DC testing

In order to verify the actual behavior at nominal power rating, the hybrid and the standard chokes were tested using a Spitzenberger Grid Simulator EMV D 45000/PAS. A 20A DC bias current with a sinusoidal component of $7.5A_{peak}$ was applied to each inductor in order to simulate the approximate conditions of a DC link choke operating in a frequency converter. Voltage and current waveform were measured and the losses were calculated. The following Table. 1. summarizes the measured data.

Nominal Power Testing			
<i>Device</i>	<i>Total Power Losses</i>	<i>Copper Losses</i>	<i>Core Losses</i>
Standard	17.24 W	13.82 W	3.42 W
Hybrid	22.04 W	18.51 W	3.53 W
Hybrid losses increment	28%	34%	3%

Table. 1. Power losses at nominal power: 20A DC bias + $7.5A_{peak}$ AC. Tested with Spitzenberger Grid Simulator EMV D 45000/PAS.

The total power losses at the nominal ratings are clearly dominated by the copper losses in both inductors. The hybrid presents 28% more total losses than the standard choke. This increment in the total losses of the hybrid is also dominated by the increase in copper losses due to the increased length and resistance of the windings.

5. Conclusions and Further Work

The saturation-gap design strategy is been presented. 50% reduction factor of the core or the winding turns is achievable with this hybrid configuration. The proposed hybrid design was simulated and physically implemented. Both, hybrid and standard inductors were empirically tested. Measurement

results show a size reduction of 50% of core volume is achieved with a small increase in losses. This increase in losses is mostly dominated by the winding resistance and it is a particularity of the design example.

MEC simulations can provide a useful view for the understanding of the saturation-gap behaviour and possibilities. On the other hand, a Finite Element Modelling, (FEM) will provide higher accuracy and the magnet tuning could be tested at the design stage.

The specific core loss mechanisms acting on the hybrid inductor are not fully identified. Core losses in standard inductors can be classified in two different types: eddy currents and hysteresis [9]. Eddy currents are produced in the magnetic core material, induced by the variations in flux. Additional eddy currents induced in the magnet are not initially expected, since the magnets are outside the coil's flux path. On the other hand, it is known that the flux level produced by a permanent magnet is dependent on the internal reluctance of the magnet and the reluctance of its magnetic path [6]. Accordingly, the permanent magnet is expected to constantly vary its flux level, following the reluctance variations in the core, inducing eddy currents within the magnet material.

Hysteresis losses are produced by friction, magnetostriction and delays in the rotation of dipoles and domains within the crystalline structure of the core [9]. The presence of the permanent magnet flux will introduce an additional tension in the domain alignment reaching an equilibrium point different from that of the core material alone. This mechanism could increase or even decrease the hysteresis losses of a given core.

A deeper analysis and experimentation dedicated to the understanding and minimization of the loss mechanism in the hybrid configuration will be the focus of further work.

6. References

- [1] Andres Revilla Aguilar and Stig Munk-Nielsen. "Method for introducing bias magnetization in ungapped cores: The Saturation-gap," APEC 2014. Unpublished.
- [2] Teruhiko Fujiwara and Hatsuo Matsumoto. "A New Downsized Large Current Choke Coil with Magnet Bias Method,". Telecommunications Energy Conference, 2003. INTELEC '03. The 25th International. 23 October 2003. IEEE, pp. 416-420.
- [3] Rafal Wrobel, Neville McNeill and Phil H. Mellor. "Design of a High-Temperature Pre-Biased Line Choke for Power Electronics Applications,". Power Electronics Specialists Conference, 2008. PESC 2008. IEEE, pp 3171 – 3177.
- [4] G.M. Shane and S.D. Sudhoff. "Permanent Magnet Inductor Design,". Electric Ship Technologies Symposium, 2011 IEEE, pp. 330-333, April 10-13, 2011.
- [5] G.M. Shane and S.D. Sudhoff. "Design and Optimization of Permanent Magnet Inductors,". Applied Power Electronics Conference and Exposition (APEC), 27th Annual IEEE, pp 1770 – 1777.
- [6] C.M. Andrews. "Understanding Permanent Magnets,". TECH Notes Group Arnold.
- [7] W.L. Soong. "BH Curve and Iron Loss Measurements for Magnetic Materials,". Power Engineering Briefing Note Series. PEBN 5. 12 May 2008
- [8] Stig Munk-Nielsen. "Experience with Spice teaching power electronics,". Power Electronics and Applications, 2009. EPE '09. 13th European Conference. IEEE, pp 1 – 8.
- [9] John B. Goodenough. "Summary of Losses in Magnetic Materials". IEEE Transactions on Magnetics. Vol. 38 NO 5 September 2002.